96 B. R. Abidi, H. Sari-Sarraf, J. S. Goddard, Jr., and M. A. Hunt, "Facet Model and Mathematical Morphology for Surface Characterization," Proc. of SPIE Conf. on Intelligent Robots and Computer Vision XVIII: Algorithms, Techniques, and Active Vision, Vol. 3837, pp. 334-344, Boston, MA, September 1999.

Facet Model and Mathematical Morphology for Surface Characterization

Besma R. Abidi, Hamed Sari-Sarraf, James S. Goddard, and Martin A. Hunt

Image Science and Machine Vision Group
Oak Ridge National Laboratory
E-mail: abidi@cyclops.ic.ornl.gov

ABSTRACT

This paper describes an algorithm for the automatic segmentation and representation of surface structures and non-uniformities in an industrial setting. The automatic image processing and analysis algorithm is developed as part of a complete on-line web characterization system of a papermaking process at the wet end. The goal is to: (1) link certain types of structures on the surface of the web to known machine parameter values, and (2) find the connection between detected structures at the beginning of the line and defects seen on the final product. Images of the pulp mixture (slurry), carried by a fast moving table, are obtained using a stroboscopic light and a CCD camera. This characterization algorithm succeeded where conventional contrast and edge detection techniques failed due to a poorly controlled environment. The images obtained have poor contrast and contain noise caused by a variety of sources.

After a number of enhancement steps, conventional segmentation methods still failed to detect any structures and are consequently discarded. Techniques tried include the Canny edge detector, the Sobel, Roberts, and Prewitt's filters, as well as zero crossings. The facet model algorithm, is then applied to the images with various parameter settings and is found to be successful in detecting the various topographic characteristics of the surface of the slurry. Pertinent topographic elements are retained and a filtered image computed. Carefully tailored morphological operators are then applied to detect and segment regions of interest. Those regions are then selected according to their size, elongation, and orientation. Their bounding rectangles are computed and represented. Also addressed in this paper are aspects of the real time implementation of this algorithm for on-line use. The algorithm is tested on over 500 images of slurry and is found to segment and characterize nonuniformities on all 500 images.

Keywords: facet model, mathematical morphology, real-time, surface characterization.

1. INTRODUCTION

On-line surface characterization of the paper web at the wet end is a very useful tool in predicting the properties and the quality of the final product. Determining the web parameters at an early stage can potentially allow the monitoring of the production events, the adjustments of the table's activity and web breaks. The feedback to industrial headbox manufacturers can also provide very valuable indications to possible flaws and a guidance to future considerations in the manufacturing process. Unfortunately, not much research is conducted on the wet end using computer vision techniques. Most of the work done on paper web inspection is applied to the dry end of the web. Both on-line and off-line, vision and non-vision techniques are tested on the dry end. The algorithm described in this paper is part of a package that would achieve the automatic, data-driven, on-line, characterization of the web surface at the wet end, using a stroboscopic light in conjunction with a CCD camera for data acquisition. Image processing and analysis techniques are used for web parameter measurements. The method using the facet model constitutes a very novel and efficient way of localizing and measuring web nonuniformities. Those non-uniformities either originate at the head box in the shape of long parallel streaks or might form and disappear at random locations on the

Part of the SPIE Conference on Intelligent Robots and Computer Vision XVIII: Algorithms, Techniques, and Active Vision Boston, Massachusetts September 1999 SPIE Vol. 3837 0277-786X/99/$10.00

surface of the web. Those streaks and structures, if persistent, can show up on the final product as non-homogeneities of the paper itself.

A number of sensors, including vision systems, have been developed for measuring paper properties both on-line[1,2] and off-line [3]. However, nearly all are intended for the dry end and typically scan across the web resulting in less that 100% web coverage. A few wet-end sensors have been proposed. Niemi has used a camera and illumination to determine the location and shape of the dry line at the wet end of a fourdrinier machine [4]. Whitaker has developed a nuclear backscatter gauge to measure consistency at the wet end [5]. This gauge samples the stock at the nip of a fourdrinier machine. Kiviranta, using stroboscopic imaging and a charge-coupled devices (CCD) camera, has investigated the role of table activity on formation in fourdrinier machines [6]. Viewing the wet end with the aid of a strobe light as a diagnostic tool is a fairly common practice in the industry. The web is usually moving at speeds of up to 6000ft/mn. This makes it impossible for the naked eye to detect any surface changes or formations. Generally, by observing the web with the help of a stroboscope, nonuniformities, flocculation, and the action of the slurry on the wire may be discerned. Aidun has used high-speed imaging to investigate the dynamics of the headbox in relation to the production of streaks and other nonuniform physical properties in paper [7]. Nomura has also used stroboscopic imaging to show the varying nonuniformities in the sheet due to variations in headbox design [8]. The headbox flow conditions have been shown to directly affect fiber orientation and other formation properties [9, 10]. While stroboscopic imaging is established as a viable on-line technique for paper web sensing, structured lighting techniques have only been used in off-line applications, such as measuring the surface roughness of paper and board [11]. In other application areas of computer vision, however, depth or range measurement using laser-based structured lighting is a well-established method [12, 13]. Image analysis and pattern recognition methodologies are also areas that have been underutilized by the paper industry researchers, especially here in the United States.

A web was first defined by Purll [14] as being any material produced in the form of strips. Textile, paper, glass, wood, metal, food, and industrial parts on a conveyor belt can all be cited under this heading. Computer tomography images were employed to detect internal defects in hardwood logs [15]. Multi-thresholding, morphological processing, and focus of attention mechanisms were used for the segmentation and recognition of the defects [16]. Ng et al. [17,18] used laser-based structured lighting in conjunction with 2-D images as a medium of data acquisition in a machine vision prototyper for the inspection of lumber webs. Color histograms were computed for color based segmentation and classification of defects. Texture analysis was also a popular way of looking and segmenting defects on wood board surfaces [19]. Graf et al. [20] used clustering and filtering software to classify sequences of defects on high quality specialty paper. Objects were classified according to their size, shape, contrast, and location. Fourier transforms and frequential analysis were applied to dry paper products for the construction of floc contour maps and the retrieval of paper grammage [21].

The algorithm developed in this paper addresses the problem of defect detection and measurement at a location of the web (wet end) rarely studied before. The computer vision technique, applied for the first time to this particular problem, achieved very satisfying results and yielded a high rate of detection as well as good accuracy of measurements.

In the following, we present the details of the developed surface characterization algorithm and illustrate its efficiency on real images of the web.

2. SURFACE CHARACTERIZATION ALGORITHM

This section presents the details of the algorithm developed for structure detection, measurement, and characterization of the surface of the slurry. The algorithm, shown in Figure 1., consists of four major steps: (1) Image enhancement and noise reduction, (2) facet model for topographic measurements and filtering of nonuniformities, (3) morphological processing for structure segmentation, and finally (4) geometric measurements and filtering.

The images to be processed are taken from an actual running paper web. The wet end of the web is photographed using a CCD camera in conjunction with a high-intensity stroboscopic light used to freeze motion. The web is traveling at 1500 ft/mn and the wire carrying the slurry is subject to other purposeful vibrations. Shaking of the table from underneath is applied via

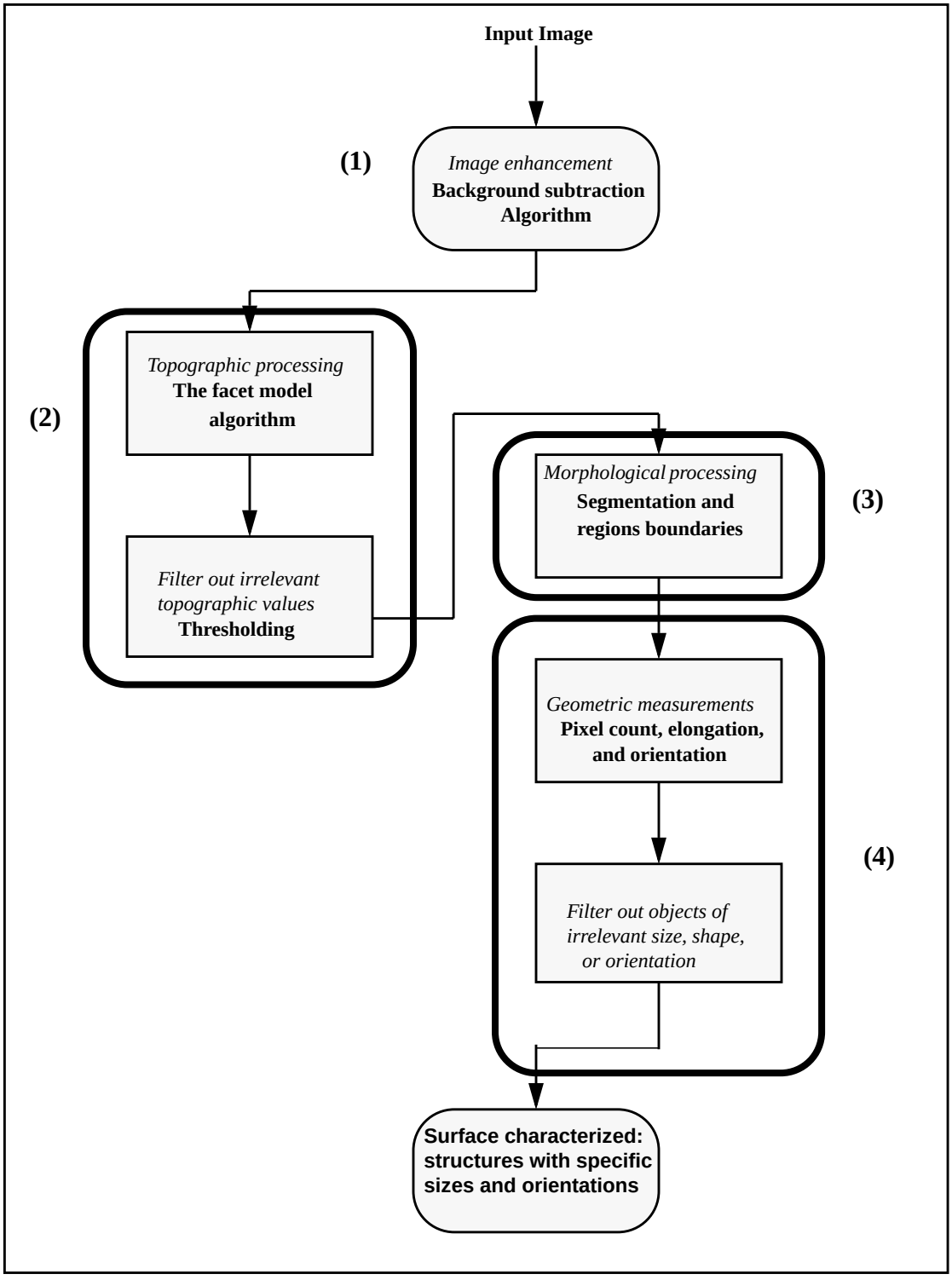

Figure 1. Block diagram of the surface characterization algorithm

metallic foils running across it. Uneven and insufficient lighting at the paper mill itself as well as the nature of the stroboscopic light and the way it is applied are of concern. Very dark images with an uneven bright spot on the side are obtained. The second artifact was caused by water beads flying over the web and generated by the shaking action of the table, therefore introducing bright spots covering large portions of the image. Figure 2 illustrates an image of the web prior to processing.

Figure 2. A raw image of the web

2.1. Image Enhancement

The raw images obtained from the web as described in section 2. merely distinguish some structure or differences in the appearance of the various regions of the slurry surface. A background subtraction algorithm is applied to enhance the appearance of the images and make them more amenable to processing and analysis. The background subtraction algorithm will be described in the following.

This process was inspired from the early work of Stanley Sternberg [22]. The essence of this routine is to remove smooth continuous backgrounds from the image. The preprocessing consists of a background removal step in which the slowly varying portion of the image is separated and then subtracted from the original image. The resulting image contains the more sharply defined features of interest. A further enhancement step then applies a histogram stretch. The background subtraction is implemented using the rolling ball method [22]. This method, based on gray scale morphology, is the same as erosion and dilation with a spherical structural element. Conceptually, consider the image as a 3-D graph where intensity is the third dimension. Then, place a ball underneath the surface of this graph and roll it under the entire image. In the case of a uniform image, the top point of the ball would be tangent to the image everywhere. Taking the locus of points defined by the topmost point of the ball as the background, the result is just the image itself. For an arbitrary image, define the topmost point of the ball at a particular (x, y) point as the background value for that point. The complete set of points forms the background image.

An important parameter influencing feature sizes in the image is the ball radius, providing a filter on the size of the image area affecting the background value. After the background image is subtracted, the remaining image generally has less dynamic range than the original. A histogram stretch is applied in which the tails are truncated to expand the dynamic range and enhance the features of interest that remain. Results of the background subtraction are shown on Figure 3.

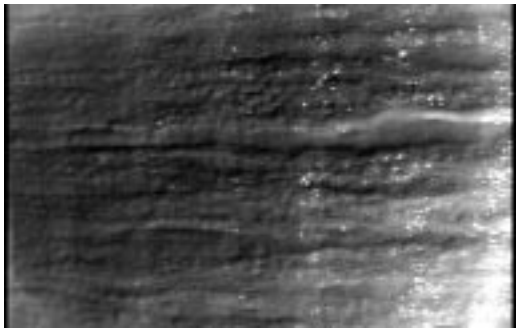

Figure 3. The background subtraction algorithm applied to the image of Figure 2.

2.2. Facet Model

The facet model is a powerful tool in image processing. Its uses range from edge detection [23,24,25], background normalization [26], shape [27] and surface topography [28], to image segmentation procedures involving detection of corners, curves, valleys, and ridges [29,30]. The facet model principle is based on the minimization of the error between the image thought of as a piecewise continuous gray level intensity surface and the observed data from the physical scene [31]. The image is considered as a noisy discretized sampling of the surface. The general forms of the facet model include piecewise constant, piecewise linear, piecewise quadratic, and piecewise cubic. In the constant model, each region in the image has a constant gray level. In the sloped model, each region has a gray level surface that is a sloped plane[29]. The model used in this work is the cubic polynomial defined by Equation (1),

$$f(x,y) = k_1 + k_2x + k_3y + k_4x^2 + k_5xy + k_6y^2 + k_7x^3 + k_8x^2y + k_9xy^2 + k_{10}y^3 \quad (1)$$

where f(x,y) is the gray level value at pixel location (x,y) whose neighborhood is to be fitted. A local vector of the 10 coefficients, computed as weighted sums of the values in the local neighborhood, is found for each pixel (x,y). A discrete orthogonal polynomial basis permits independent estimation of each coefficient as a linear combination of the data values in the neighborhood of (x,y). Those polynomials are given by Equation (2) for the 1-D case. The 2-D polynomials are obtained by taking the tensor product of the 2 sets of 1-D polynomials.

Let the discrete integer index set R be symmetric in the sense that $r \in R$ implies $-r \in R$. Let $P_n(r)$ be the n^{th} order polynomial. The discrete polynomials are iteratively constructed as follows:

Define $P_0(r) = 1$. Suppose $P_0(r), \ldots, P_{n-1}(r)$ have been defined.

$$P_n(r) = r^n + a_{n-1}r^{n-1} + \ldots + a_1r + a_0. \quad (2)$$

$P_n(r)$ must be orthogonal to each polynomial $P_0(r), \ldots, P_{n-1}(r)$. We then have the set of n linear equations

$$\sum_{r \in R} P_k(r)\left(r^n + a_{n-1}r^{n-1} + \ldots + a_1r + a_0\right) = 0, k = 0, \ldots, n-1 \quad (3)$$

Solving for the set of equations yields the set of discrete orthogonal polynomials

$$P_{i+1}(r) = rP_i(r) - \beta_iP_{i-1}(r) \quad (4)$$

where,

$$\beta_i = \frac{\sum r P_i(r) P_{i-1}(r)}{\sum_{r \in R} P_{i-1}(r^2)} \qquad (5)$$
$$P_0(r) = 1, P_1(r) = r$$

The first five polynomials are given as

$$P_0(r) = 1$$
$$P_1(r) = r$$
$$P_2(r) = r^2 - \frac{\mu_2}{\mu_0} \qquad (6)$$
$$P_3 = r^3 - \left(\frac{\mu_4}{\mu_2} \cdot r\right)$$
$$P_4 = r^4 + \frac{(\mu_2)\mu_4 - \mu_0\mu_6)r^2 + \mu_2\mu_6 - \mu^2{}_4}{\mu_0\mu_4 - \mu^2{}_2}$$

where $\mu_k = \sum_{s \in R} s^k$.

The facet model consists of solving an equal weighted least square fitting problem by minimizing the error

$$e^2 = \sum_{r \in R} \left[d(r) - \sum_{n=0}^{K} a_n P_n(r) \right]^2 \qquad (7)$$

in terms of the a_n coefficients. d(r) is the data value observed (grey level values). The coefficients of the bivariate cubic of Equation (1), $k_1, k_2, \ldots, k_n$ can then be determined. An error image describing the quality of fit is also generated. Given the 10 coefficients k_i defining the polynomial at pixel location (x,y), a number of topographic measurements can be determined. Image intensity surface patches are labeled and grouped according to the categories defined by monotonic, gray level, and invariant functions of directional derivatives, namely the gradient and the Hessian of the facets given by Equation (8).

$$\begin{bmatrix} \frac{\partial f}{\partial x} \\ \frac{\partial f}{\partial y} \end{bmatrix} \text{ and } \begin{bmatrix} \frac{\partial^2 f}{\partial x^2} \frac{\partial^2 f}{\partial x \partial y} \\ \frac{\partial^2 f}{\partial y \partial x} \frac{\partial^2 f}{\partial y^2} \end{bmatrix} \qquad (8)$$

The signs of those quantities are used to identify the region's label. This results in the following categories: (1) Peak, (2) Ridge, (3) Saddle, (4) Flat, (5) Ravine, (6) Pit, (7) concave Hillside, (8) Saddle Hillside, (9) slope Hillside, and (10) convex Hillside. The image can then be represented in a rich and hierarchical structure using these topographic units. The topographic structures properties are defined in [16]. The facet model coefficients were computed for images of the wet end of the paper web using a window size of 13×13. Smaller size windows were also tested and were found not to yield good results. Comparative images with window sizes of 5×5 and *13 x 13* are shown in Figure 4.

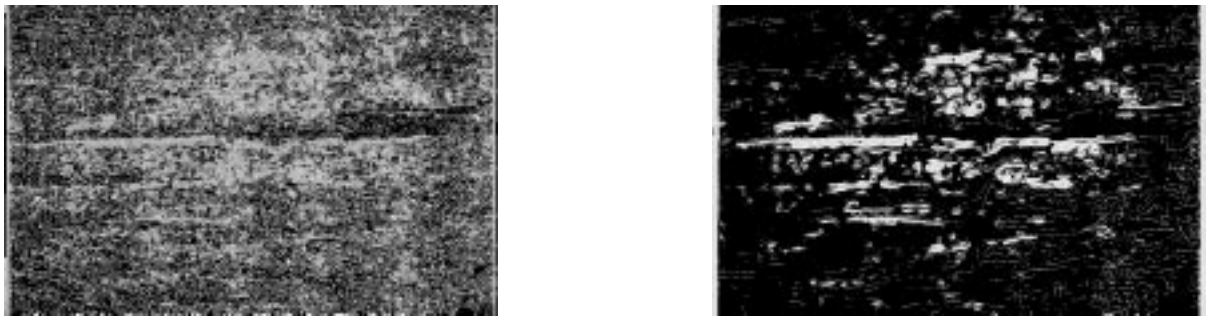

(a) (b)

Figure 4. Topographic images using (a) 5x5 window and (b) 13x13 window.

It is noticeable from the results of the facet model that a number of elongated structures with distinguishable topographic characteristics are present. From our observations on more than 500 processed images, the nonuniformities seem to have certain common topographic characteristics. Values that are of the types: hillside convex, hillside concave, and hillside saddle all yield a good characterization of the structures in question. Based on those observations, a multilevel thresholding was applied to the topographic images where only those values corresponding to hillsides (concave, convex, saddle) were retained.

2.3. Mathematical Morphology for Binary Image segmentation

Using the image in Figure 4(b), a binary version is computed by leaving only the hillsides (concave, convex, and saddle). That image still contains some noise and small size components and needs some further cleaning. Morphological processing is used towards the filtering of small size features and the segmentation of the image. A closing with a structuring element in the horizontal direction followed by an opening with the same structuring element are applied. The results of this operation are shown in Figure 5.

Figure 5. Filtering of elongated structures using morphological operators.

A closing followed by an erosion is subtracted from the dilated version of the same image to yield a set of boundaries of the various structures in the image, see Figure 6. The objects resulting from the morphological processing were then filtered according to their size, orientation, and elongation. Figure 7 shows the result of that operation and represents the characterization of the surface of the slurry using minimum bounding rectangles (MBR) to identify the nonuniformities.

Figure 6. Binary and boundary images of the slurry.

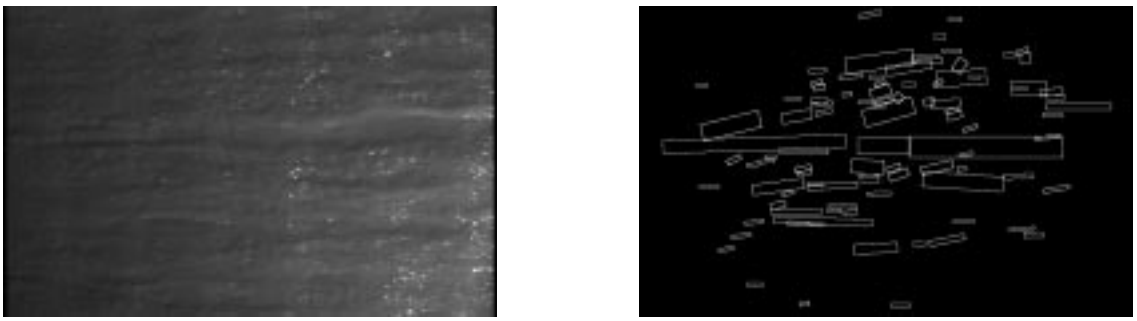

(a) (b)

Figure 7. (a) Original image of the slurry, (b) results of the surface characterization algorithm(MBR).

3. Real-Time Implementation of the Facet Model

A real-time facet model implementation is being developed for computing the surface feature parameters at *30* frames per second. This implementation is on a Detachable Maxpci containing dedicated pipeline processing hardware for image processing applications. An initial design has been completed in which the necessary computations have been mapped to the hardware. Figures 8 and 9 show a block diagram of the design. The cubic polynomial approximation consists of ten terms with coefficients k_1 through k_{10}. Each coefficient is calculated by convolving the input image with a mask. The mask is predetermined to compute the least square fit of the Chebyshev polynomials to the input image. On the Datacube board, dedicated convolution hardware is used for this computation. These computations are performed at 40 Mhz., so that a 512 x 512 image will require 7 ms. for each coefficient calculation. With a 100-point convolver, two convolutions can be performed at the same time with up to a 7 x 7 convolution mask. The total time for the coefficient calculations is approximately 35 ms. After convolution, the coefficients are stored in memory and are used in the next step of the parameter calculations. Using the arithmetic blocks and look-up tables, the gradient, the gradient magnitude, the eigenvalues and eigenvectors of the Hessian are calculated. From these quantities the various feature values can be determined.

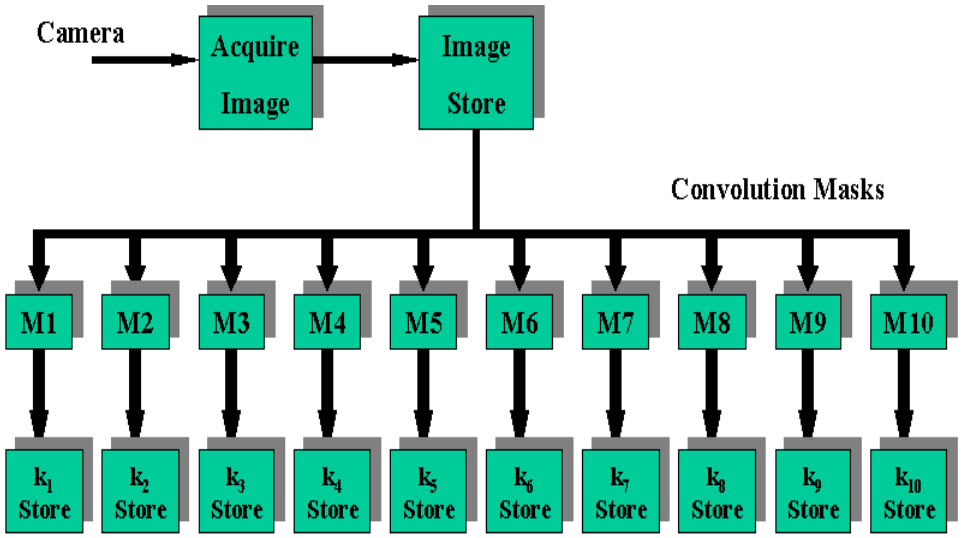

Figure 8. Block diagram of the real-time implementation of the facet model

4. Conclusion and Future Work

In this paper, we propose a new application for the facet model algorithm. We show that the surface of a paper web at the wet end can be characterized using image enhancement algorithms (the background subtraction) followed by topographic descriptions via the facet model. Mathematical morphology is then used for the final segmentation of the results. Geometric filtering yields well-segmented images with clearly defined nonuniformities. Measurements of location, size, and orientation of the structures are also computed. The initial work on the real-time implementation of the facet model is addressed. The algorithm implemented yields a very good rate of detection of the nonuniformities on the surface of the web. Future work will involve the use of a laser-based structured light profiler in conjunction [32] with the CCD camera in order to study the third dimension of the web not represented by the 2-D images.

References

[1] K. Humphrey, *Image Analysis*, Pira International, 1995.
[2] S. I. Shapiro and R. H. Shearin, “On-Line Sensors: Exploring the Trends,” *Tappi Journal*, **78**, No. 9, pp. 83-84, September 1995.
[3] J.-P. Bernie and W. J. M. Douglas, “Local Grammage Distribution and Formation of Paper by Light Transmission Image Analysis,” *Tappi Journal*, **79**, No. 1, pp. 193-202, January 1996.
[4] A. J. Niemi, and C. J. Backstrom, “Automatic Observation of Dry Line on Wire for Wet End Control of the Paper Machine,” *Pulp and Paper Canada*, **95**, no. 2, pp. 27-30, February 1994.
[5] M. Whitaker, “Optimizing Formation Through Consistency Measurement - a Wet End Revolution,” *Paper Technology*, **36**, no. 2, pp. 22-26, March 1995.
[6] A. Kiviranta, “The Role of Table Activity in Fourdrinier Forming,” Canadian Pulp and Paper Association 79th Annual Meeting Technical Section, Montreal, Canada, January 1993.
[7] C. K. Aidun, “Hydrodynamics of Streaks on the Forming Table,” *Tappi Journal*, August 1997.
[8] T. Nomura, K. Wada, and T. Shimizu, “High Consistency Sheet Forming,” *Tappi Journal*, pp. 115-122, January 1989.

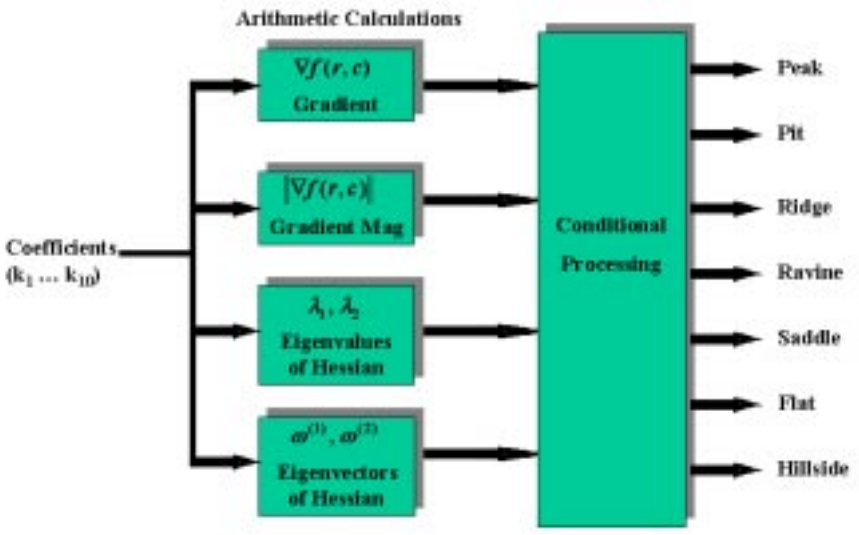

Figure 9. Block diagram of the real-time implementation of the facet model (continued)

[9] H. Dahl, H. Holik, and E. Weisshuhn, “The Influence of Headbox Flow Conditions on Paper Properties and Their Constancy,” *Tappi Journal*, pp. 93-98, February 1988.
[10] C. K. Aidun and A. E. Kovacs, “Hydrodynamics of the Forming Section: The Origin of Nonuniform Fiber Orientation,” *Tappi Journal*, **78**, No. 11, November 1995.
[11] S. I’Anson, “3-D Laser Surface Profiling of Paper and Board,” *Paper Technology*, **38**, no. 2, pp. 43-49, March 1997.
[12] T. A. Vuori and C. L. Smith, “Three-Dimensional Imaging System with Structured Lighting and Practical Constraints,” *Journal of Electronic Imaging*, **6**, No. 1, pp. 140-144, January 1997.
[13] H. Kaplan, “Structured Light Finds a Home in Machine Vision,” *Photonics Spectra*, January 1994.
[14] D. J. Purll, “Solid State Image Sensors in Automated Visual Inspection”, B. G. Batchelor, D. A. Hill and D. C. Hodgson, Eds., Elsevier Science Publishing Company, Inc., New York, NY, pp. 255-293, 1985.
[15] D. Zhu and A. A. Louis Beex, “Robust Spatial Autoregressive Modeling for Hardwood Texture Analysis”, *Journal of Visual Communication and Image Representation*, **36**, no. 9,, September 1993, Academic Press.
[16] P. Araman, D. Schmoldt, T. H. Cho, D. Zhu, R. Conners, and D. Earl Kline,” Machine Vision Systems for Processing Hardwood Lumber and Logs”, *AI Applications*, **6**, no. 2, April 1992, pp. 13-26.
[17] C. T. Ng, R. W. Conners, and P. A. Araman, “An Experimental Machine Vision Prototyper for the Inspection of Planar Webs”, Proc. of the twenty fourth Southeastern Symposium on System Theory, March 1-3 1992, pp. 483-487.
[18] R. W. Conners, C. T. Ng. T. H. Cho, and C. W. McMillin, “Computer Vision System for Locating and Identifying Defects in Hardwood Lumber”, Proc. of the SPIE, vol. 1095, 1989, pp. 48-63.
[19] C. W. Kim and A. J. Koivo, “Hierarchical Classification of Surfaced Defects on Dusty Wooden Boards”, Proc. of 10th. Int’l. Conf. on Pattern Recognition, 1990, pp. 775-779.
[20] J. E. Graf, S. T. Enright, and S. I. Shapiro,” Automated Web Inspection Ensures Highest Quality Nonwovens”, *Tappi Journal*, **78**, no. 9, September 1995, pp. 135-138.
[21] J. P. Bernie and W. J. Murray Douglas, “Local Grammage Distribution and Formation of Paper by Light Transmission Image Analysis”, *Tappi Journal*, **79**, no. 1, January 1996, pp. 193-202.
[22] S. R. Sternberg, “Biological Image Processing”, *Computer*, January 1983, pp. 22-34.
[23] A. Rangarajan, R. Chellappa, and Y. T. Zhou, A model-based approach for filtering and edge detection in noisy images, *IEEE Trans. on Circuits and Systems*, **37**, pp. 140-144, 1990.

[24] E. P. Lyvers, O. R. Michell, M. L. Akey, and A. P. Reeves, “Subpixel Measurement Using Moment Based Edge Operator”, IEEE Trans. PAMI, **12**, pp. 1293-1309, 1989.
[25] H. Jiang and Y. Cai, “Edge Detection from Surface Fitting by Orthogonal Polynomial”, *Acta Automatica Sinica*, **16**, pp. 202-209, 1990.
[26] M. Jankowski, “An Iterated Facet Model Approach to Background Normalization”, Proc. of the SPIE, **2238**, pp. 198-206, 1994.
[27] C. P. Ting, R. M. Haralick, and L. G. Shapiro, “Shape from Shading Using Facet Model”, *Pattern Recognition*, **22**, pp. 683-695, 1989.
[28] Q. Zheng and R. Chellappa, “Estimation of Surface Topography from Stereo SAR Images”, IEEE ICASSP-89, Glasgow, UK, **3**, pp. 1614-1617, 1989.
[29] R. M. Haralick and L. G. Shapiro,” Computer and Robot Vision”, Addison Wesley Publishing Company, Inc., 1st ed., 1992.
[30] P. I. Radeva, “A Rule-based Approach to Hand X-ray Image Segmentation”, Computer Analysis of Images and Patterns, 5th Int’l. Conf., CIAP 93 Proc., Budapest, Hungary, pp. 641-648, 1993.
[31] S. D. Pathak, Y. Kim, and J. Kim, “Efficient Implementation of Facet Models on a Multimedia System”, *Optical Engineering*, **35**, pp. 1739-1745, 1996.
[32] H. Sari-Sarraf, J. S. Goddard, Jr., J. C. Turner, M. A. Hunt, and B. R. Abidi, “On-Line Characterization of Slurry for Monitoring Headbox Performance”, Tappi Proc., Milwaukee, WI, 1998, pp. 97-115.